European Journal of Medicinal Chemistry 237 (2022) 114374

Contents lists available at ScienceDirect

European Journal of Medicinal Chemistry

journal homepage: http://www.elsevier.com/locate/ejmech

The azulene scaffold from a medicinal chemist's perspective: Physicochemical and *in vitro* parameters relevant for drug discovery

Teppo O. Leino [a, b], Peter Sieger [c], Jari Yli-Kauhaluoma [a], Erik A.A. Wallén [a], Jörg T. Kley [d, *]

[a] Drug Research Program, Division of Pharmaceutical Chemistry and Technology, Faculty of Pharmacy, University of Helsinki, P.O. Box 56, FI-00014, Finland
[b] Department of Chemistry and NanoScience Center, University of Jyväskylä, P.O. Box 35, FI-40014, Jyväskylä, Finland
[c] Boehringer Ingelheim Pharma GmbH & Co. KG, Drug Discovery Sciences Germany, Birkendorfer Straße 65, 88397, Biberach an der Riß, Germany
[d] Boehringer Ingelheim Pharma GmbH & Co. KG, Medicinal Chemistry Germany, Birkendorfer Straße 65, 88397, Biberach an der Riß, Germany

ARTICLE INFO

Article history:
Received 11 March 2022
Received in revised form
5 April 2022
Accepted 7 April 2022
Available online 12 April 2022

Keywords:
Azulene
Indole
Naphthalene
Photostability
Scaffold hopping

ABSTRACT

Azulene is a bicyclic scaffold rarely applied in medicinal chemistry. Here we report physicochemical and *in vitro* parameters relevant for drug discovery for a series of diversely substituted azulenes. We synthesized and characterized several scaffold hopping series of analogously substituted azulenes, indoles and naphthalenes. This enabled a comparison of azulene with the more common scaffolds indole and naphthalene. Our data indicates that undesirably low photostability of azulenes is restricted to certain substitution patterns. Generally, we conclude that azulene is an underused lipophilic bicycle and should be considered as a valuable complement to the collection of medicinal chemistry scaffolds.

1. Introduction

Azulene (**1**) is a bicyclic non-benzenoid aromatic hydrocarbon, a structural isomer of naphthalene (**2**). Despite the structural resemblance, the physicochemical properties of these compounds differ considerably from each other. Azulene has a dipole moment between the electron-rich five-membered ring and the electron-deficient seven-membered ring [1], and it exhibits a characteristic deep blue color [2], whereas naphthalene is colorless and does not possess dipole moment between the rings. The aromatic heterocycles indole and azulene both consist of an electron-rich five-membered ring fused to a larger ring. From this angle, azulene can be considered to be an isostere of indole (**3**).

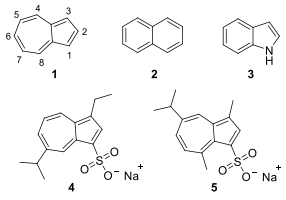

Azulene derivatives have attracted only scant attention in medicinal chemistry research [3], unlike the aforementioned scaffolds naphthalene and indole [4]. Antiulcer drugs egualen sodium (**4**) and sodium gualenate (**5**) are the only azulene-based drugs on the market so far [5]. Other reported bioactivities of azulene derivatives include anticancer [6–8], anti-inflammatory [9], antidiabetic [10], antimicrobial [11,12], and antifungal [13] effects, orexin receptor activation and potentiation of orexin-A [14,15], thromboxane A_2 (TXA_2) antagonism [16–18], and dopamine D4 activation [19,20]. In addition, both azulene and its alkyl substituted derivative guaiazulene have been investigated for use in photodynamic therapy [21–23].

The characteristic electron distribution of azulene has a significant impact on its reactivity. The reactivity, in turn, greatly contributes to the synthetically accessible functionalization pattern of azulene. The most nucleophilic positions of the ring system are 1 and 3, which can be easily functionalized applying electrophilic aromatic substitution reactions [24,25]. In case these positions are already substituted, the weakly nucleophilic 5- and 7-positions may react with electrophiles [26,27]. On the contrary, the 4-, 6- and 8-positions of azulene have been reported to react with nucleophiles [28,29]. The 2-position may be selectively functionalized through transition metal-catalysed C–H activation methods [30–32].

* Corresponding author.
E-mail address: joerg.kley@boehringer-ingelheim.com (J.T. Kley).

https://doi.org/10.1016/j.ejmech.2022.114374

The electron distribution also affects the metabolism of azulene, as cytochrome P450 (CYP) enzymes typically oxidize electron-rich positions of aromatic rings [33]. The sulphate conjugate of 1-hydroxyazulene has been identified as the main metabolite of azulene in rats [34], confirming that oxidation of azulene mainly occurs at its most electron-rich position. However, 1-hydroxyazulene itself has been reported to be too unstable to be isolated [35].

Sufficient metabolic stability is a prerequisite for achieving sufficient exposure in target organs upon administration of a drug molecule. Therefore, reducing electron density especially at the five-membered ring is an obvious strategy to improve the metabolic stability of azulenes, which can be approached by introducing an electron-withdrawing group (EWG). Functionalization of the 1- and 3-position with EWGs can be carried out by aromatic electrophilic substitution reactions: Vilsmeier-Haack reaction gives a formyl substituent and the modified Vilsmeier-Haack or Friedel-Crafts acylation affords ketone derivatives (Scheme 1) [25,36]. The carboxyl group and the respective esters and amides can be obtained via acid chloride using phosgene [15]. Alternatively, the carboxylic acid can be reached using trifluoroacetic anhydride followed by basic hydrolysis [37]. Compared to the 1- and 3-positions, synthetic methods to substitute the 2-position of azulene with EWGs have been less explored. One approach is the functionalization via boronic acid pinacol ester [30], which can be further converted to carbonyl derivatives [38].

The introduction of an EWG on the seven-membered ring could also result in reducing potential metabolic liabilities, as it lowers the overall electron density of the aromatic system. However, the functionalization of the seven-membered ring with EWGs is less straightforward than the five-membered ring, as the reports of substitution methods are scarce. Often the most convenient approach to functionalize the seven-membered ring is to synthesize the azulene ring from simple starting materials with methods, which selectively direct the desired substituents or precursors to the seven-membered ring in the azulene ring construction step [39–44]. A methyl group in the 4-, 6- or 8-position is an example of a versatile precursor in the synthesis of EWGs, as it can be easily converted to the carbonyl derivative via enamine intermediate (Scheme 1) [14,45,46].

In this study we explored the general potential of azulene as a scaffold in medicinal chemistry by determining the physicochemical and *in vitro* parameters relevant for drug discovery for a series of azulene derivatives. Additionally, we compared the azulene derivatives to their corresponding indole and naphthalene analogs in order to reveal differences between these analogous bicyclic scaffolds.

2. Results and discussion

2.1. Selection and design of compound series

The compound properties relevant for drug discovery result from the combination of the scaffold and its substituents. In order to allow a meaningful assessment of azulene as a scaffold for medicinal chemistry, we studied a series of azulenes bearing electronically diverse substituents at different positions of the ring. To this end, compounds with demonstrated biological activity described in the literature [14,15] were complemented by azulene derivatives newly synthesized through known methodologies (for a complete list see Table S1 and section 2 in Supporting Information).

To compare the azulene scaffold with naphthalene and indole, we established and tested a total of 15 scaffold hopping series, each characterized by a specific substituent pattern (section 2.4, Table 5). *N*-Alkylated indoles are considerably more lipophilic than their counterparts displaying the NH proton. For the comparison of scaffolds, we therefore kept these two types of indoles separate.

2.2. Stability

Decomposition of azulenes has been reported to occur at high temperature and upon irradiation [47–49]. Furthermore, the marketed drug sodium gualenate (**5**) is known to decompose upon storage at ambient temperature even as solid [50]. We investigated whether instability of azulenes is general or depending on substitution. To this end, we tested sets of representative azulene derivatives in assays routinely applied at Boehringer Ingelheim for the characterization of leads and during lead optimization. This allowed us to assess the degree of instability under conditions relevant for medicinal chemistry and drug development.

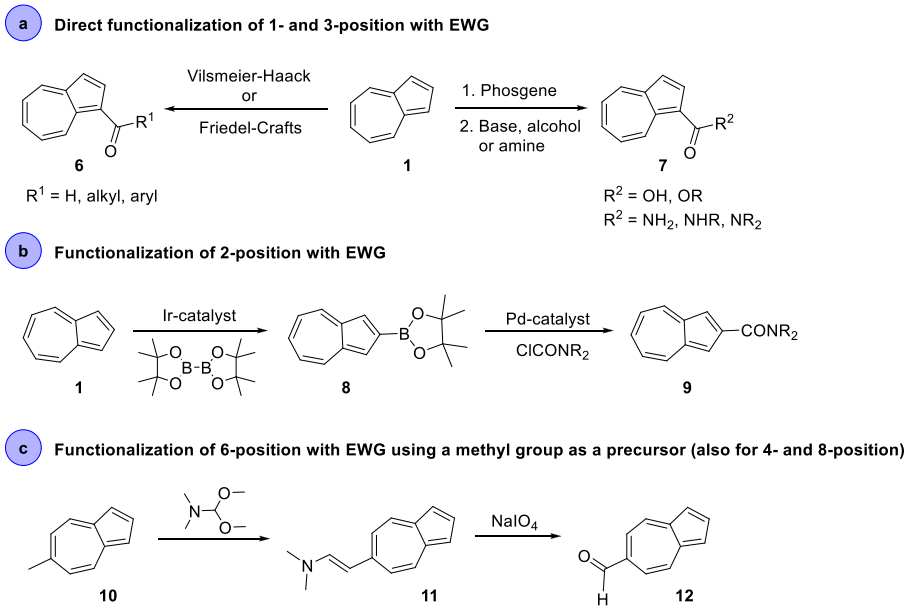

Scheme 1. Functionalization the azulene scaffold with an electron-withdrawing group (EWG).

2.2.1. Hydrolytic stability

Taking into account that substituent effects might influence hydrolytic stability, we tested a set of four azulenes bearing substituents with different electronic properties at different positions (Table 1). None of the compounds showed signs of instability under pH 7.4 conditions (3 days at 40 °C). Decomposition was detected for three out of the four compounds when strongly acidic conditions were applied (a 0.1 M solution of HCl in H_2O, 3 days at 40 °C). However, even the least stable compound **14** with an electron donating acylamino substituent in 2-position, remained 96.5% unchanged. These data indicate more than sufficient hydrolytic stability for solid form development (e.g., tablet, capsule) with no need for protection against the acidic gastric environment.

2.2.2. Photostability

Rapid degradation of azulene and guaiazulene under harsh UV light conditions has been reported [48,49]. We observed that also an azulene with an electron withdrawing substituent (carboxamide 13) is highly unstable under Suntester conditions (see section 3.2 in Supporting Information). Analogs of 13 with an indole or naphthalene scaffold (compounds **17**, **18**, **19**) were stable under these conditions, indicating that the observed instability is associated with the azulene scaffold itself (Table 2).

Whether the absorption of light in the UV–vis region and the concomitant generation of degradation products from the parent compound azulene [48] is associated with photomutagenicity, photogenotoxicity or phototoxicity has been investigated by Struwe et al. From a cell-based assessment they conclude that azulene is neither photomutagenic nor photogenotoxic, and it shows only weak photo(cyto)toxicity [51]. The mechanism underlying the phototoxic effects of azulene and guaiazulene is most likely the generation of reactive oxygen species (ROS) upon irradiation with UVA light [52]. A number of successfully marketed drug molecules are sensitive to UV light [53] and testing under milder irradiation conditions is required to judge whether the degree of photolability of a compound is acceptable for drug development or not. Using the light sensitive drug nifedipine (20) as a reference, compounds (either as solid or in solution) were exposed to sunlight for 7 days on a windowsill in uncolored glass vials. We emphasize that this method is not standardized, and results will vary to a certain extent, mainly depending on the intensity of sunlight during the period of exposure. Nevertheless, this approach should allow a meaningful ranking of compounds even when tested on different weeks, provided half-lives differ by more than one or two orders of magnitude.

We tested a set of 8 sufficiently soluble substituted azulenes bearing electron withdrawing, electron donating or electronically neutral substituents at different positions of the core and the comparator nifedipine (Table 3). No photodegradation from solid was detected for any of the compounds tested (<0.5% degradation). When tested in solution, photodegradation above the detection limit (0.5% degradation) was seen for 5 of the azulene derivatives and for nifedipine. Interestingly, the most electron-rich azulene (14) bearing an acylamino moiety in 2-position proved to be the least stable one showing 85% degradation after 7 days, corresponding to a half-life in the range of 2–3 days (ca. 60 h). The half-life of the reference compound nifedipine was determined to be approximately 4 min (ca. 1/15 h), almost three orders of magnitude shorter.

Based on assay conditions relevant for drug development, our results show that photostability of azulenes strongly depends on the substituent pattern with half-lives spanning several orders of

Table 1
Hydrolytic stability of the selected compounds.

Entry	Compound	Structure	Hydrolytic stability	
			Decomposition after 3 d at 40 °C in 0.1 M aq. HCl*	Decomposition after 3 d at 40 °C in aq. buffer pH 7.4*
1	13	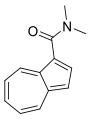	<0.5%	<0.5%
2	14	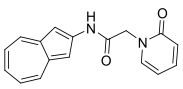	3.5%	<0.5%
3	15	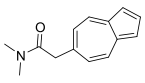	2.0%	<0.5%
4	16	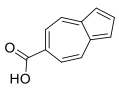	1.5%	<0.5%

* Visual inspection indicated complete dissolution under the applied conditions.

Table 2
Photostability (suntester conditions) of the selected compounds.

Compound	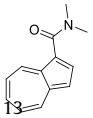 13	 17	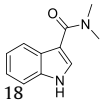 18	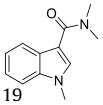 19	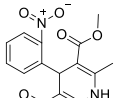 Nifedipine (20)
Photostability (suntester) % degradation 24 h at UV stress	100%	<0.5%	<0.5%	<0.5%	100%

Table 3
Photostability (mild conditions) of the selected compounds.

Entry	Compound	Structure	Photostability	
			% degradation from solid 7 d "mild"	% degradation in solution[*1] 7 d "mild" (intrinsic pH of solution)
1	13	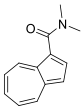	<0.5%	3% (pH 8.6)
2	14	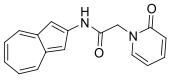	<0.5%	85%[*2] (pH 7.1)
3	15	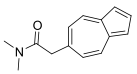	<0.5%	12% (pH 5.3)
4	16	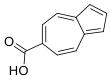	<0.5%	<0.5% (pH 4.0)
5	21	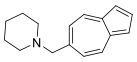	<0.5%	3.5% (pH 8.7)
6	22	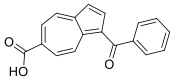	<0.5%	<0.5% (pH 4.1)
7	23	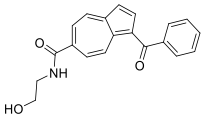	<0.5%	<0.5% (pH 5.8)
8	24	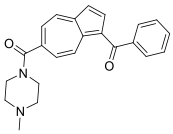	<0.5%	<0.5% (pH 7.2)
9	Nifedipine (20)	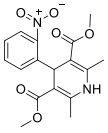	n.d.	100% (t½~4min)

n.d. = not determined.
[*1] Acetonitrile/water 40:60.
[*2] Analysis by HPLC detecting absorption at 375 nM (main absorption peak of azulene). The decay of the compound peak upon irradiation is not accompanied by the occurrence of new peaks with absorbance at 375 nM, indicating that the azulene moiety of the molecule is decomposed rather than the pyridone moiety.

magnitude. Noteworthy, even our least stable azulene derivative proved more stable than the marketed drug nifedipine.

2.3. Safety

In order to detect potential safety issues inherently associated with the azulene core, we tested representative compounds for cytotoxicity, inhibition of CYP enzymes and reactivity towards glutathione.

2.3.1. Cytotoxicity

The three compounds (**13**, **27**, **28**) tested in an MTT cytotoxicity assay using HepG2 cells showed no signs of cytotoxicity up to 400 μM, the highest concentration tested (Table 4).

2.3.2. Inhibition of CYP enzymes

Aiming at minimizing the risk of clinical drug-drug interactions, inhibition of CYP enzymes is an unwanted feature of potential drug candidates [54]. Accordingly, the need for abolishing CYP inhibition – where required – adds an additional layer of complexity to lead optimization programs. Lead molecules devoid of this liability are therefore preferred. We tested a diverse set of 11 azulenes for inhibition of the CYP isoenzymes 2C9, 2C8, 2D6, 2C19, and 3A4. Apart from two single-digit μM IC_{50} values (**21** against CYP2C19 and **29** against CYP2C8), all IC_{50} values were above 10 μM with no detectable inhibition in most cases (Table 4).

2.3.3. GSH stability

Determination of compound stability in the presence of the biologically relevant nucleophile glutathione (GSH) is an established method to determine the reactivity of covalent reactive groups [55]. In order to rule out unwanted covalent reactivity, we tested a set of azulene derivatives with different substitution patterns in a GSH assay (**13**, **14**, **15**, **16**, **22**, **30**; structures are shown in Supporting Information Table S1). All compounds were stable in the presence of glutathione (half-life >1000 h). For comparison, the half-life of ritlecitinib (**31**), a weakly reactive covalent JAK3 inhibitor, was 32 h under our assay conditions.

Table 4
Cytotoxicity and inhibition of CYP enzymes of the selected compounds.

Entry	Compound	Structure	Cytotoxicity (μM)	Inhibition of CYP enzymes, IC_{50} (μM)				
				2C9	2C8	2D6	2C19	3A4
1	13	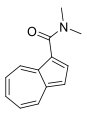	>400	>50	>50	>50	>50	>50
2	21	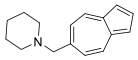	n.d.	>50	>50	17	2.3	>50
3	22	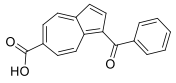	n.d.	>50	>50	>50	>50	>50
4	23	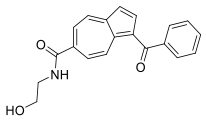	n.d.	>50	>50	>50	>50	>50
5	24	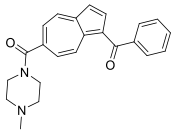	n.d.	39	>50	>50	>50	>50
6	**25**	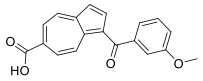	n.d.	>50	22	>50	>50	>50
7	**26**	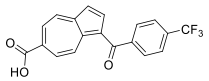	n.d.	>50	13	>50	>50	>50
8	**27**	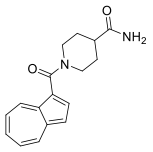	>400	>50	>50	>50	>50	>50
9	**28**	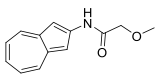	>400	>50	>50	>50	22	>50
10	**29**	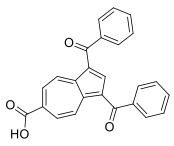	n.d.	12	1.5	>50	>50	>50

n.d. = not determined.

2.4. Comparison of the azulene scaffold with indole and naphthalene

The aromatic hydrocarbon azulene is a valence isomer of naphthalene. Compared to naphthalene, the lower symmetry of azulene (both geometrically and electronically) gives rise to a rich diversity of potential molecules that can be accessed via chemistries partly not applicable to the naphthalene core. As a bicyclic aromatic system with an electron-rich five-membered ring, azulene can also be considered as an isostere of indole. Here we compare azulene with naphthalene and indole scaffolds, considering the properties relevant for medicinal chemistry. To allow a meaningful comparison of azulenes, we prepared scaffold hopping series each comprising direct analogs with naphthalene and/or indole core decorated with the same functionalities. Our comparison considers both *N*-methylated indoles (which share the same number of non-hydrogen atoms and the absence of a donor hydrogen with their azulene analogs) and the respective non-methylated analogs. The compounds were grouped in 15 series based on the substitution patterns and the experimental values of each compound series are shown in Table 5.

2.4.1. Polarity

The existence of its dipole moment (1.08 D in benzene) [1] suggests that azulene is more polar than naphthalene. However, in terms of LogP the difference is only 0.2 log units (median based on our data from 4 pairs of direct analogs: series A, B, C, E; range: 0.0−0.2 log units, Table 5). In contrast, azulenes are considerably less polar than the corresponding *N*-methylindoles. Our data from 12 compound pairs make a median difference of 0.8 log units

Table 5
The results of polarity, permeability, solubility, and metabolic stability with human liver microsomes determination experiments of compound series **A**–**O**.[1]

Series	Compound	Structure	logP[2]	PAMPA Permeability ($\times 10^{-6}$ cm/s)	Solubility (μg/ml)			Metabolic stability with HLM (% QH)
					pH 2.2	pH 4.5	pH 6.8	
A	13	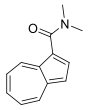	1.6	7.6	>43	>44	>40	67
	17		1.8	8.3	>47	>50	>43	<23
	18		0.4	2.2	>47	>47	>44	25
	19	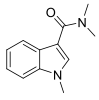	1.3	6.7	>51	>51	>51	55
B	**27**	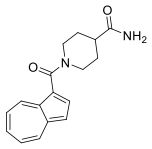	0.6	0.5	>71	>57	>58	<23
	32	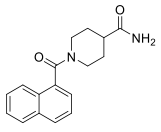	0.8	0.2	>70	>71	>71	<23
	33	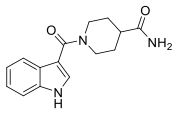	−0.2	<0.01	n.d.	n.d.	n.d.	<23
	34	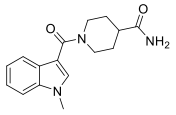	0.4	0.2	>71	44	>64	<23
C	**15**	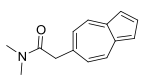	2.2	8.7	>44	>45	>43	27
	35	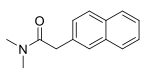	2.4	4.7	41	39	40	40
	36	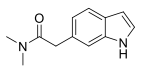	1.0	1.3	>51	>51	>51	<23
	37	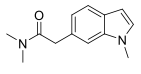	1.7	7.6	>54	>53	>53	<23
D	**21**	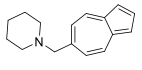	>5.5	3.4	>56	41	31	75
	38	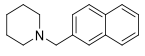	>5.5	4.6	34	30	27	72
E	**39**	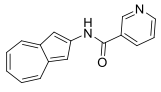	2.4	4.8	43	3	2	71

Table 5 (*continued*)

Series	Compound	Structure	logP[2]	PAMPA Permeability ($\times 10^{-6}$ cm/s)	Solubility (μg/ml)			Metabolic stability with HLM (% QH)
					pH 2.2	pH 4.5	pH 6.8	
	40	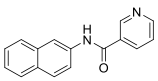	2.4	5.5	>50	6	4	67
	41	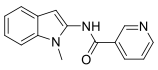	1.3	4.9	>59	n.d.	n.d.	23
F	**14**	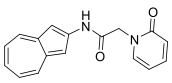	1.7	3.7	4	2	2	<23
	42	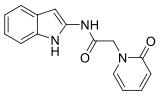	0.4	0.1	>60	>67	>67	<23
	43	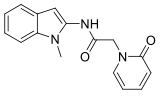	1.1	3.3	n.d.	n.d.	3	<23
G	**30**	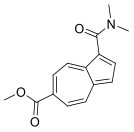	2.1	7.4	>64	50	>64	n.d.
	44	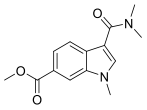	1.4	4.2	50	>52	49	82
H	**45**	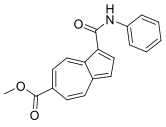	3.8	0.4	<1	<1	<1	n.d.
	46	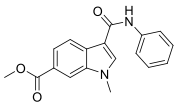	2.9	2.2	<1	<1	<1	n.d.
I	**47**	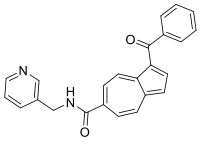	3.0	2.4	70	<1	<1	46
	48	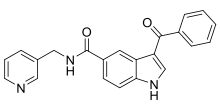	1.4	0.1	>79	1	<1	56
	49	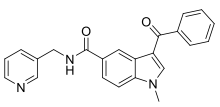	2.1	1.7	81	3	<1	<23
J	**23**	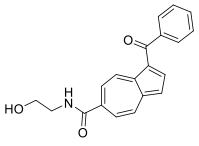	2.2	1.8	14	6	4	<23

(*continued on next page*)

Table 5 (*continued*)

Series	Compound	Structure	logP[2]	PAMPA Permeability ($\times 10^{-6}$ cm/s)	Solubility (μg/ml)			Metabolic stability with HLM (% QH)
					pH 2.2	pH 4.5	pH 6.8	
	50	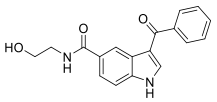	0.6	0.01	39	18	15	53
	51	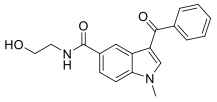	1.3	0.5	53	66	45	<23
K	**24**	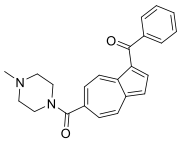	3.0	8.4	>90	67	>73	48
	52	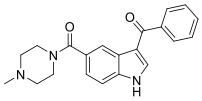	1.3	0.2	>74	>75	69	<23
	53	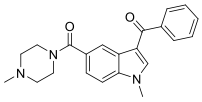	2.0	1.9	78	76	68	<23
L	**54**	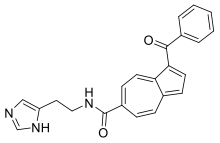	2.3	0.3	>77	57	<1	41
	55	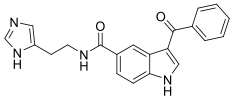	0.8	<0.01	>81	>78	66	<23
	56	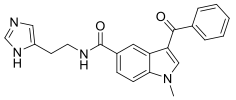	1.5	0.1	84	107	72	<23
M	**57**	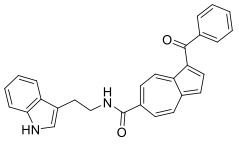	4.3	0.03	<1	<1	<1	69
	58	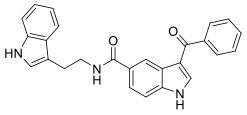	2.8	<0.01	<1	<1	1	84
	59	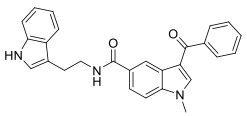	3.5	0.04	<1	<1	<1	79
N	**60**	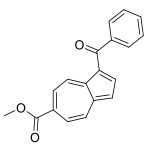	4.7	0.1	<1	<1	<1	n.d.

Table 5 (*continued*)

Series	Compound	Structure	logP[2]	PAMPA Permeability ($\times 10^{-6}$ cm/s)	Solubility (μg/ml)			Metabolic stability with HLM (% QH)
					pH 2.2	pH 4.5	pH 6.8	
	61	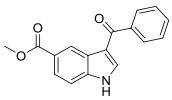	2.5	2.8	<1	<1	<1	n.d.
	62	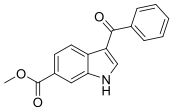	2.7	1.5	<1	<1	<1	n.d.
	63	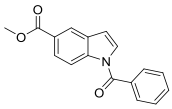	4.4	0.5	<1	<1	<1	n.d.
	64	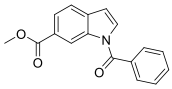	4.3	0.5	<1	<1	<1	n.d.
O	**65**	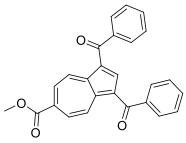	5.5	0.3	<1	<1	<1	n.d.
	66	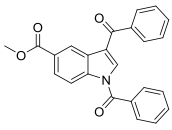	5.2	1.3	<1	<1	<1	n.d.
	67	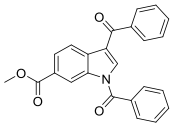	5.2	2.1	<1	<1	<1	n.d.

[1] Respective experimental data for further compounds beyond the scaffold hopping series from this table are given in the Supporting Information (Table S6).
[2] Calculated from experimental HPLC retention times (see section 3.6 in Supporting Information). n.d. = not determined.

(series A, B, C, E, F, G, H, I, J, K, L, M; range 0.2–1.1 log units, Table 5). As expected, the indole scaffold with unsubstituted NH is the most polar among our reference scaffolds: the logP difference to azulenes is 1.5 (median from 11 compound pairs; series A, B, C, F, I, J, K, L, M, N, N; range: 0.8–2.2 log units, Table 5). The change of median lipophilicity upon replacing the azulene scaffold with *N*-methylindole or naphthalene is visualized in Fig. 1.

2.4.2. Permeability

PAMPA permeability within the scaffold hopping series is largely governed by logP. As a rule, azulenes permeate faster than the respective indoles and show similar permeability as their naphthalene analogs (Fig. 2).

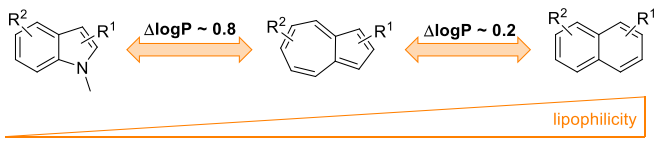

Fig. 1. Median lipophilicity differences between *N*-methylindole, azulene and naphthalene derivatives. Lipophilicity increases from left to right.

2.4.3. Solubility

Within several of our scaffold hopping series, solubility is either generally above the highest concentration tested (i.e., >250 μM; series A and B in Table 5) or generally below the detection limit of the high throughput assay applied (series H, M, N, O in Table 5). The limited amount of data from the other scaffold hopping series do not indicate a clear trend for superior or inferior solubility of the respective azulene derivatives.

2.4.4. Metabolic stability

A comparison of compound stability upon incubation with human liver microsomes (HLM) reveals cases of marked difference within the series, e.g., in series A and series J (Table 5). There is, however, no general trend indicating superior or inferior metabolic stability of the azulene series over the respective indoles or naphthalenes.

2.4.5. Pharmacokinetic properties of carboxylates of azulene, naphthalene and indole

Pharmacokinetic properties of acidic drug molecules are strongly influenced by the pK_a value of the acidic group present in the molecule [56]. Generally, strongly acidic molecules tend to be

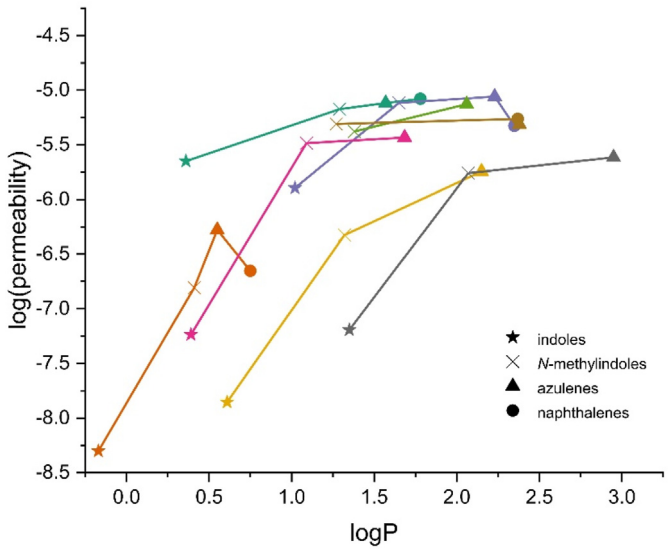

Fig. 2. logP vs. permeability. In each scaffold hopping series the indole derivative is located on bottom-left (lower permeability and higher polarity) and its azulene and naphthalene analogs are close to each other in top-right (higher permeability and lower polarity). Each symbol represents one scaffold: asterisk = indole, cross = *N*-methylindole, triangle = azulene, circle = naphthalene. Compounds in the same series connected with line and each series have own color: cyan = series A, orange = series B, purple = series C, brown = series E, pink = series F, green = series G, dark grey = series I, yellow = series J. Series D, H, K, L, M, N, O have been excluded from the figure: Compounds in series D, K, L may have a different degree of protonation at the pH of PAMPA measurement (pH 7.4). Permeability data of series H, M, N, O may contain artefacts as solubilities of compounds from these series are below the detection limit.

poorly absorbed, as the fraction of the more permeable uncharged species becomes negligible at intestinal pH. Interestingly, there is no oral drug molecule with a naphthalenecarboxylate scaffold reported to have entered clinical development (adapalene, a retinoic acid receptor agonist with naphthalene-2-carboxylate core, has been developed for topical application) [57]. In contrast, three oral drugs based on the less acidic indole-3-carboxylate scaffold have entered clinical development (PF-06409577 (AMPK stimulator, terminated after clinical phase 1); LY-2562175 (FXR agonist, terminated after clinical phase 1); TM-30510 (GPR-44 antagonist; PGD2 antagonist, terminated after clinical phase 1). Indole-3-carboxylic acid (**69**) and azulene-1-carboxylic acid (**68**) have their carboxylate moieties positioned at the electron-rich five-membered ring resulting in very similar and relatively high pK_a values, 5.29 and 5.1, respectively (Supporting Information, Table S4). This suggests that azulene-1-carboxylic acid (just as indole-3-carboxylic acid) should be a scaffold suited for oral acidic drug molecules. In contrast and not unexpectedly, azulene-6-carboxylic acid (**16**) with its carboxylate positioned at the electron-deficient 7-membered ring, is even more acidic than the two naphthoic acid isomers (pK_a = 3.5; Supporting Information, Table S4).

2.4.6. Intellectual property considerations

Compared to indoles and naphthalenes, azulene derivatives are much less prominent in chemical literature, including patent literature. For both indoles and naphthalenes the number of published compounds is more than 100-fold the number of azulenes (see Supporting Information, Table S5). The numerical ratio of patent applications covering example compounds with the respective cores is in the same range. Novelty should therefore be much easier to achieve with azulenes than with compounds based on an indole or a naphthalene core.

3. Conclusions

Stability and safety related data generated from our set of variously substituted azulenes contradict general liabilities of the azulene scaffold. Photostability of azulenes with novel substitution patterns, however, should be monitored early on, especially when electron donating substituents are applied.

Despite the dipole moment present, substituted azulenes are only marginally more polar than their naphthalene analogs. Accordingly, naphthalenes and azulenes show comparable permeability, while their significantly more polar indole analogs are consistently less permeable. Discrepancies within the scaffold hopping series concerning aqueous solubility and stability in human liver microsomes do not follow general trends.

Altogether, we consider azulene as an underexplored lipophilic scaffold without general relevant liability, and our experimental data argue against excluding the azulene moiety from the treasure chest of medicinal chemistry scaffolds. The scarce presence of azulene-based compounds in literature, including patent literature, even increases the attractiveness of azulene as a scaffold in medicinal chemistry.

Author contributions

T.O.L. and J.T.K. designed the study. T.O.L., J.Y.K., E.A.A.W. and J.T.K. contributed in the compound synthesis and T.O.L., P.S. and J.T.K. analyzed and interpreted the data. The manuscript was written through contributions of all authors. All authors have given approval to the final version of the manuscript.

Declaration of competing interest

The authors declare that they have no known competing financial interests or personal relationships that could have appeared to influence the work reported in this paper.

Acknowledgements

T.O.L. acknowledges the Academy of Finland (grant no. 330800) and the Doctoral Programme in Drug Research of the University of Helsinki for financial support.

The authors thank Keith Graham for valuable discussions.

Appendix A. Supplementary data

Supplementary data to this article can be found online at https://doi.org/10.1016/j.ejmech.2022.114374.

Abbreviations

CYP	cytochrome P450
GSH	γ-L-glutamyl-L-cysteinylglycine (glutathione)
HLM	human liver microsomes
IP	intellectual property
MTT	3-(4,5-dimethylthiazol-2-yl)-2,5-diphenyltetrazolium bromide
n.d.	not determined
PAMPA	parallel artificial membrane permeability assay

References

[1] J.A.G. Anderson, B.M. Steckler, A study of the visible absorption spectra and dipole moments of some 1- and 1,3-substituted azulenes, J. Am. Chem. Soc. 81 (18) (1959) 4941–4946, https://doi.org/10.1021/ja01527a046.

[2] R.S.H. Liu, A.E. Asato, Tuning the color and excited state properties of the azulenic chromophore: NIR absorbing pigments and materials, J. Photochem.

Photobiol. C Photochem. Rev. 4 (3) (2003) 179–194.
[3] P. Bakun, B. Czarczynska-Goslinska, T. Goslinski, S. Lijewski, In vitro and in vivo biological activities of azulene derivatives with potential applications in medicine, Med. Chem. Res. 30 (4) (2021) 834–846, https://doi.org/10.1007/s00044-021-02701-0.
[4] N. Chadha, O. Silakari, Indoles as therapeutics of interest in medicinal chemistry: bird's eye view, Eur. J. Med. Chem. 134 (Supplement C) (2017) 159–184.
[5] Takashi Yanagisawa, Shuichi Wakabayashi, Tsuyoshi Tomiyama, Masafumi Yasunami, K. Takase, Synthesis and anti-ulcer activities of sodium alkylazulene sulfonates, Chem. Pharm. Bull. 36 (2) (1988) 641–647.
[6] A.E. Asato, A. Peng, M.Z. Hossain, T. Mirzadegan, J.S. Bertram, Azulenic retinoids: novel nonbenzenoid aromatic retinoids with anticancer activity, J. Med. Chem. 36 (21) (1993) 3137–3147, https://doi.org/10.1021/jm00073a013.
[7] C.-H. Chen, O. Lee, C.-N. Yao, M.-Y. Chuang, Y.-L. Chang, M.-H. Chang, Y.-F. Wen, W.-H. Yang, C.-H. Ko, N.-T. Chou, et al., Novel azulene-based derivatives as potent multi-receptor tyrosine kinase inhibitors, Bioorg. Med. Chem. Lett 20 (20) (2010) 6129–6132.
[8] B.-C. Hong, Y.-F. Jiang, E.S. Kumar, Microwave-assisted [6+4]-Cycloaddition of fulvenes and α-pyrones to azulene–indoles: facile syntheses of novel antineoplastic agents, Bioorg. Med. Chem. Lett 11 (15) (2001) 1981–1984, https://doi.org/10.1016/S0960-894X(01)00349-3.
[9] F. Ayaz, A. Yuzer, T. Ince, M. Ince, Anti-cancer and anti-inflammatory activities of bromo- and cyano-substituted azulene derivatives, Inflammation 43 (3) (2020) 1009–1018, https://doi.org/10.1007/s10753-020-01186-0.
[10] K. Ikegai, M. Imamura, T. Suzuki, K. Nakanishi, T. Murakami, E. Kurosaki, A. Noda, Y. Kobayashi, M. Yokota, T. Koide, et al., Synthesis and biological evaluation of C-glucosides with azulene rings as selective SGLT2 inhibitors for the treatment of type 2 diabetes mellitus: discovery of YM543, Bioorg. Med. Chem. 21 (13) (2013) 3934–3948, https://doi.org/10.1016/j.bmc.2013.03.067.
[11] J. Peet, A. Selyutina, A. Bredihhin, Antiretroviral (HIV-1) activity of azulene derivatives, Bioorg. Med. Chem. 24 (8) (2016) 1653–1657, https://doi.org/10.1016/j.bmc.2016.02.038.
[12] M. Feussi Tala, J. Qin, J.T. Ndongo, H. Laatsch, New azulene-type sesquiterpenoids from the fruiting bodies of lactarius deliciosus, Nat. Prod. Bioprospect. 7 (3) (2017) 269–273, https://doi.org/10.1007/s13659-017-0130-1.
[13] T. Murafuji, K. Kitagawa, D. Yoshimatsu, K. Kondo, K. Ishiguro, R. Tsunashima, I. Miyakawa, Y. Mikata, Heterocyclic bismuth carboxylates based on a diphenyl sulfone scaffold: synthesis and antifungal activity against Saccharomyces cerevisiae, Eur. J. Med. Chem. 63 (2013) 531–535, https://doi.org/10.1016/j.ejmech.2013.02.036.
[14] T.O. Leino, A. Turku, J. Yli-Kauhaluoma, J.P. Kukkonen, H. Xhaard, E.A.A. Wallén, Azulene-based compounds for targeting orexin receptors, Eur. J. Med. Chem. 108 (2018) 88–100.
[15] A. Turku, T.O. Leino, L. Karhu, J. Yli-Kauhaluoma, J.P. Kukkonen, E.A.A. Wallén, H. Xhaard, Structure–activity relationships of 1-benzoylazulenes at the OX1 and OX2 orexin receptors, ChemMedChem 14 (9) (2019) 965–981, https://doi.org/10.1002/cmdc/201900074.
[16] T. Tomiyama, S. Wakabayashi, K. Kosakai, M. Yokota, Azulene derivatives: new non-prostanoid thromboxane A2 receptor antagonists, J. Med. Chem. 33 (9) (1990) 2323–2326, https://doi.org/10.1021/jm00171a004.
[17] T. Tomiyama, M. Yokota, S. Wakabayashi, K. Kosakai, T. Yanagisawa, Design, synthesis, and pharmacology of 3-substituted sodium azulene-1-sulfontes and related compounds: non-prostanoid thromboxane A2 receptor antagonists, J. Med. Chem. 36 (7) (1993) 791–800, https://doi.org/10.1021/jm00059a001.
[18] M. Yokota, S. Uchibori, H. Hayashi, R. Koyama, K. Kosakai, S. Wakabayashi, T. Tomiyama, Azulene derivatives as TXA2/PGH2 receptor antagonists—II. Synthesis and biological activity of 6-mono- and 6-dihydroxylated-isopropylazulenes, Bioorg. Med. Chem. 4 (4) (1996) 575–591, 10.1016/0968-0896(96)00038-7.
[19] S. Löber, N. Tschammer, H. Hübner, M.R. Melis, A. Argiolas, P. Gmeiner, The azulene framework as a novel arene bioisostere: design of potent dopamine D4 receptor ligands inducing penile erection, ChemMedChem 4 (3) (2009) 325–328, https://doi.org/10.1002/cmdc.200800395.
[20] S. Löber, H. Hübner, A. Buschauer, F. Sanna, A. Argiolas, M.R. Melis, P. Gmeiner, Novel azulene derivatives for the treatment of erectile dysfunction, Bioorg. Med. Chem. Lett 22 (23) (2012) 7151–7154, https://doi.org/10.1016/j.bmcl.2012.09.064.
[21] T. Damrongrungruang, N. Kitchindaopat, P. Thanasothon, K. Theeranut, P. Tippayawat, C. Ruangsuwan, B. Suwannee, Effects of photodynamic therapy with azulene on peripheral blood mononuclear cell viability and singlet oxygen formation, Photodiagnosis Photodyn. Ther. 24 (2018) 318–323, https://doi.org/10.1016/j.pdpdt.2018.10.015.
[22] A. Phutim-Mangkhalthon, A. Teerakapong, P. Tippayawat, N.P. Morales, S. Morkmued, S. Puasiri, A. Priprem, T. Damrongrungruang, Anti-inflammatory effect of photodynamic therapy using guaiazulene and red lasers on peripheral blood mononuclear cells, Photodiagnosis Photodyn. Ther. 31 (2020) 101747, https://doi.org/10.1016/j.pdpdt.2020.101747.
[23] T. Damrongrungruang, S. Rattanayatikul, N. Sontikan, B. Wuttirak, A. Teerakapong, A. Kaewrawang, Effect of different irradiation modes of azulene-mediated photodynamic therapy on singlet oxygen and PGE2 formation, Photochem. Photobiol. 97 (2) (2021) 427–434, https://doi.org/10.1111/php.13346.
[24] M. Kędziorek, P. Mayer, H. Mayr, Nucleophilic reactivities of azulene and fulvenes, Eur. J. Org Chem. (8) (2009) 1202–1206, https://doi.org/10.1002/ejoc.200801099, 2009.
[25] A.G. Anderson, J.A. Nelson, Tazuma, J.J. Azulene III., Electrophilic substitution, J. Am. Chem. Soc. 75 (20) (1953) 4980–4989, https://doi.org/10.1021/ja01116a030.
[26] K. Hafner, K.-L. Moritz, Zur Kenntnis Der Azulene XIII, Elektrophile substitutionen des azulens in 2- und 5- bzw. 7-stellung, Justus Liebigs Ann. Chem. 656 (1) (1962) 40–53, https://doi.org/10.1002/jlac.19626560108.
[27] T. Shoji, S. Ito, M. Watanabe, K. Toyota, M. Yasunami, N. Morita, Synthesis of 5-heteroarylazulenes: first selective electrophilic substitution at the 5-position of azulene, Tetrahedron Lett. 48 (17) (2007) 3009–3012, https://doi.org/10.1016/j.tetlet.2007.02.110.
[28] S. Hünig, K. Hafner, B. Ort, M. Müller, Einführung funktioneller gruppen in den siebengliedrigen ring des azulens, Liebigs Ann. Chem. (7) (1986) 1222–1240, https://doi.org/10.1002/jlac.198619860708, 1986.
[29] Y. Fukazawa, S. Usui, Y. Kurate, Y. Takeda, N. Saito, Nucleophilic reaction of azulene derivatives with some ketone enolates, J. Org. Chem. 54 (12) (1989) 2982–2985, https://doi.org/10.1021/jo00273a043.
[30] K. Kurotobi, M. Miyauchi, K. Takakura, T. Murafuji, Y. Sugihara, Direct introduction of a boryl substituent into the 2-position of azulene: application of the miyaura and smith methods to azulene, 2003, Eur. J. Org Chem. (18) (2003) 3663–3665, https://doi.org/10.1002/ejoc.200300001.
[31] M. Murai, K. Takami, H. Takeshima, K. Takai, Iridium-catalyzed dehydrogenative silylation of azulenes based on regioselective C–H bond activation, Org. Lett. 17 (7) (2015) 1798–1801, https://doi.org/10.1021/acs.orglett.5b00575.
[32] Z.M. Png, T.L.D. Tam, J. Xu, Carboxylic acid directed C–H arylation of azulene, Org. Lett. 22 (13) (2020) 5009–5013, https://doi.org/10.1021/acs.orglett.0c01576.
[33] P.R. Lazzara, T.W. Moore, Scaffold-hopping as a strategy to address metabolic liabilities of aromatic compounds, RSC Med. Chem. 11 (1) (2020) 18–29, https://doi.org/10.1039/C9MD00396G.
[34] R.P. Hanzlik, P. Bhatia, Metabolism of azulene in rats, Xenobiotica 11 (11) (1981) 779–783, https://doi.org/10.3109/00498258109045882.
[35] T. Asao, S. Ito, N. Morita, 1-Hydroxyazulene and 3-hydroxyguaiazulene: synthesis and their properties, Tetrahedron Lett. 30 (48) (1989) 6693–6696, https://doi.org/10.1016/S0040-4039(00)70653-8.
[36] K. Hafner, C. Bernhard, Zur kenntnis der azulene, IV: azulen-aldehyde und -ketone, Justus Liebigs Ann. Chem. 625 (1) (1959) 108–123, https://doi.org/10.1002/jlac.19596250116.
[37] A.G. Anderson, R.G. Anderson, The reaction of azulenes with trifluoro- and trichloroacetic anhydride, J. Org. Chem. 27 (10) (1962) 3578–3581, https://doi.org/10.1021/jo01057a044.
[38] M. Fujinaga, K. Suetake, K. Gyoji, T. Murafuji, K. Kurotobi, Y. Sugihara, An easy access to 2-substituted azulenes from azulene-2-boronic acid pinacol ester, Synthesis (23) (2008) 3745–3748, 2008.
[39] K. Hafner, Zur kenntnis der azulene I. Eine neue azulen-synthese, Justus Liebigs Ann. Chem. 606 (1) (1957) 79–89, https://doi.org/10.1002/jlac.19576060109.
[40] K. Rudolf, D. Robinette, T. Koenig, Synthesis, characterization and flash vacuum pyrolysis studies of anti-[2.2](1,6)Azulenophane, J. Org. Chem. 52 (4) (1987) 641–647, https://doi.org/10.1021/jo00380a027.
[41] T. Nozoe, S. Seto, S. Matsumura, T. Asano, Synthesis of azulene derivatives from troponoids and cyanoacetic ester, Proc. Jpn. Acad. 32 (5) (1956) 339–343.
[42] R. Yokoyama, S. Ito, M. Watanabe, N. Harada, C. Kabuto, N. Morita, [2 + 2] cycloaddition reaction of cycloheptatriene with dichloroketene. A novel and efficient synthetic strategy for the synthesis of 2-hydroxyazulene, J. Chem. Soc. Perkin Trans. 1 (18) (2001) 2257–2261, https://doi.org/10.1039/B104164A.
[43] S. Carret, A. Blanc, Y. Coquerel, M. Berthod, A.E. Greene, J.-P. Deprés, Approach to the blues: a highly flexible route to the azulenes, Angew. Chem. Int. Ed. 44 (32) (2005) 5130–5133, https://doi.org/10.1002/anie.200501276.
[44] A.L. Crombie, J.L. Kane, K.M. Shea, R.L. Danheiser, Ring expansion-annulation strategy for the synthesis of substituted azulenes and oligoazulenes. 2. Synthesis of azulenyl halides, sulfonates, and azulenylmetal compounds and their application in transition-metal-mediated coupling reactions, J. Org. Chem. 69 (25) (2004) 8652–8667, https://doi.org/10.1021/jo048698c.
[45] K. Kurotobi, K.S. Kim, S.B. Noh, D. Kim, A. Osuka, A quadruply azulene-fused porphyrin with intense near-IR absorption and a large two-photon absorption cross section, Angew. Chem. Int. Ed. 45 (24) (2006) 3944–3947, https://doi.org/10.1002/anie.200600892.
[46] G.E. Williams, G. Kociok-Köhn, T.D. James, S.E. Lewis, C4-Aldehyde of guaiazulene: synthesis and derivatisation, Org. Biomol. Chem. 19 (11) (2021) 2502–2511, https://doi.org/10.1039/D0OB02567D.
[47] L.T. Scott, M.A. Kirms, Azulene thermal rearrangements. Carbon-13 labeling studies of automerization and isomerization to naphthalene, J. Am. Chem. Soc. 103 (19) (1981) 5875–5879, https://doi.org/10.1021/ja00409a042.
[48] J.I. Selco, T. Brooks, M. Chang, M.T. Trieu, J.K. McDonald, S.P. McManus, Solution photochemistry of azulene, J. Org. Chem. 59 (2) (1994) 429–433, https://doi.org/10.1021/jo00081a024.
[49] J. Fiori, R. Gotti, A. Albini, V. Cavrini, Study on the photostability of guaiazulene by high-performance liquid chromatography/mass spectrometry and gas chromatography/mass spectrometry, Rapid Commun. Mass Spectrom. 22 (17) (2008) 2698–2706, https://doi.org/10.1002/rcm.3661.
[50] K. Nakamichi, T. Nakano, H. Yasuura, S. Izumi, Y. Kawashima, Stabilization of sodium guaiazulene sulfonate in granules for tableting prepared using a twin-

screw extruder, Eur. J. Pharm. Biopharm. 56 (3) (2003) 347–354, https://doi.org/10.1016/S0939-6411(03)00100-0.
[51] M. Struwe, M. Csato, T. Singer, E. Gocke, Comprehensive assessment of the photomutagenicity, photogenotoxicity and photo(Cyto)Toxicity of azulene, Mutat. Res. Toxicol. Environ. Mutagen. 723 (2) (2011) 129–133, https://doi.org/10.1016/j.mrgentox.2011.03.017.
[52] H.-M. Chiang, J.-J. Yin, Q. Xia, Y. Zhao, P.P. Fu, K.-C. Wen, H. Yu, Photo-irradiation of azulene and guaiazulene—formation of reactive oxygen species and induction of lipid peroxidation, J. Photochem. Photobiol. Chem. 211 (2) (2010) 123–128, https://doi.org/10.1016/j.jphotochem.2010.02.007.
[53] R. de Vries, L. Diels, L. Dillen, L. Sips, D. Van Roosbroek, T. Verhaeghe, P. Timmerman, Assessment of light stability of drugs in blood and plasma, Bioanalysis 8 (19) (2016) 2007–2021, https://doi.org/10.4155/bio-2016-0109.
[54] S.T.M. Orr, S.L. Ripp, T.E. Ballard, J.L. Henderson, D.O. Scott, R.S. Obach, H. Sun, A.S. Kalgutkar, Mechanism-based inactivation (MBI) of cytochrome P450 enzymes: structure–activity relationships and discovery strategies to mitigate drug–drug interaction risks, J. Med. Chem. 55 (11) (2012) 4896–4933, https://doi.org/10.1021/jm300065h.
[55] M.E. Flanagan, J.A. Abramite, D.P. Anderson, A. Aulabaugh, U.P. Dahal, A.M. Gilbert, C. Li, J. Montgomery, S.R. Oppenheimer, T. Ryder, et al., Chemical and computational methods for the characterization of covalent reactive groups for the prospective design of irreversible inhibitors, J. Med. Chem. 57 (23) (2014) 10072–10079, https://doi.org/10.1021/jm501412a.
[56] E. Proschak, P. Heitel, L. Kalinowsky, D. Merk, Opportunities and challenges for fatty acid mimetics in drug discovery, J. Med. Chem. 60 (13) (2017) 5235–5266, https://doi.org/10.1021/acs.jmedchem.6b01287.
[57] G.E. Piérard, C. Piérard-Franchimont, P. Paquet, P. Quatresooz, Spotlight on Adapalene. Expert Opin. Drug Metab. Toxicol. 5 (12) (2009) 1565–1575, https://doi.org/10.1517/17425250903386269.